Chemo-enzymatic synthesis of [2-^{13}C, 7-^{15}N]-ATP for facile NMR analysis of RNA

Lukasz T. Olenginski ● Theodore K. Dayie

Received: ……/Accepted …

Abstract We report the efficient chemo-enzymatic synthesis of an [2-^{13}C, 7-^{15}N]-adenosine 5'-triphosphate building block for incorporation into RNA via T7 RNA polymerase-based *in vitro* transcription. Such atom-specific labeling alleviates spectral crowding and simplifies the analysis of large RNAs by solution NMR spectroscopy. Applications to probe adenosine C2 and N7 sites in a large 61 nucleotide viral RNA with two- and three-dimensional NMR experiments are demonstrated.

Keywords Nucleotides ● Nucleic acids ● Isotopic labeling ● Spectroscopy

✉ Theodore K. Dayie
dayie@umd.edu

[1] Center for Biomolecular Structure and Organization, Department of Chemistry and Biochemistry, University of Maryland, College Park, MD 20742, United States.

Introduction

Solution nuclear magnetic resonance (NMR) spectroscopy is a powerful biophysical technique capable of probing RNA structure and dynamics at high-resolution [1–4]. A prerequisite for contemporary NMR analysis is the introduction of stable isotope (e.g. ^{2}H, ^{13}C, ^{15}N, and ^{19}F) labels into RNA [5–13]. This is most commonly achieved with isotope labeled ribonucleoside 5'-triphosphates (rNTPs) and T7 RNA polymerase (RNAP)-based *in vitro* transcription (IVT) [14–17]. These rNTPs can either be uniformly ^{2}H, ^{13}C, ^{15}N, or ^{13}C/^{15}N or atom-specifically (e.g. adenosine ^{13}C2) labeled. The former is commercially available whereas the latter must be prepared in-house. Numerous reports on the synthesis of atom-specifically labeled rNTPs by biomass fermentation [18–21] or complete *de novo* synthesis [22–24] exist in the literature. However, these procedures either require laborious enzyme cloning, expression, and purification or lengthy chemical synthesis schemes.

We have recently described our preferred synthetic routes for rNTPs with [8-^{13}C]-adenine (A), [8-^{13}C]-guanine (G), [6-^{13}C, 1,3-$^{15}N_2$]-uracil (U), and [6-^{13}C, 1,3-$^{15}N_2$]-cytosine labeling to permit simplified resonance assignment strategies [25] and artefact-free dynamics probing [26–28]. Our approach combines chemical nucleobase synthesis with enzymatic ribose

coupling and subsequent phosphorylation [27–29]. Importantly, this is achieved with fewer enzymes and synthetic steps and at lower costs compared to other labeling approaches [18–24]. Our method is compatible with chemically synthesized or commercially available nucleobase and ribose and yields a versatile assortment of atom-specifically labeled rNTPs. Although a number of ^{13}C and/or ^{15}N-labeled adenine derivatives are known [30–37], the specific combination of [2-^{13}C, 7-^{15}N]-adenine has only been reported by Moody and co-workers to study toyocamycin biosynthesis [36]. However, this labeling pattern has yet to be implemented in the corresponding rNTP building block for use in IVT of RNA.

This particular nucleobase labeling is advantageous for NMR analysis to detect canonical or noncanonical base pair interactions and ligand binding that occur on the Watson-Crick (C2) or Hoogsteen (N7) face of adenosine residues. This is especially true for large RNAs with complex folding or ligand interactions where spectral crowding complicates resonance assignment. Additionally, the removal of ^{13}C and ^{15}N dipolar coupling partners permits straightforward and accurate probing of RNA dynamics [18, 20, 26, 38]. Here, we present a chemo-enzymatic procedure to synthesize [2-^{13}C, 7-^{15}N]-ATP. Applications to probe adenosine C2 and N7 sites in a large 61 nucleotide (nt) viral RNA [39, 40] with two (2D)- and three (3D)-dimensional NMR experiments are demonstrated. Importantly, these

experiments can be readily adapted to any RNA of interest for facile NMR analysis of structure, dynamics, and ligand interactions.

Results and Discussion

Synthesis

The atom-specifically labeled [2-^{13}C, 7-^{15}N]-ATP **8** was assembled with a hybrid chemical and enzymatic approach (Scheme 1). First, we chemically synthesized [2-^{13}C, 7-^{15}N]-adenine **7** following previous protocols [31, 36]. Several routes to ^{15}N-labeled adenine initiate from di- or triaminopyrimidines [32, 37] but they were not adopted in the present study due to our desired ^{13}C(2) labeling.

Scheme 1

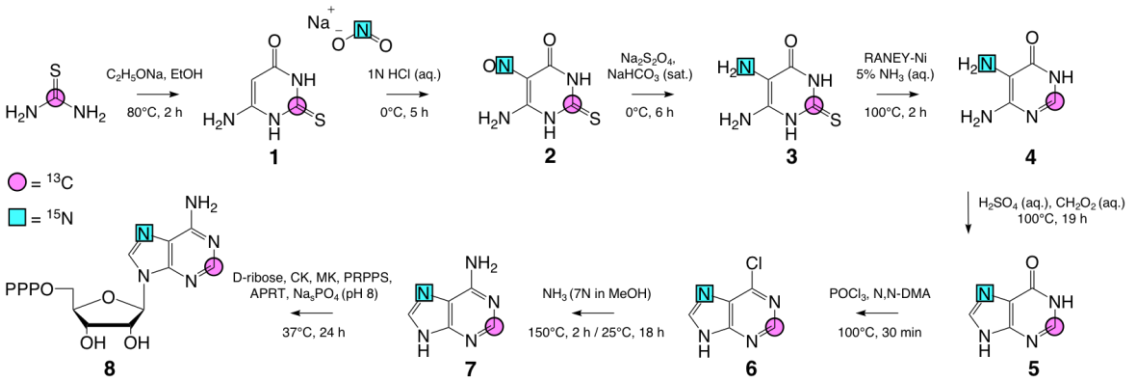

We therefore employed a sodium ethoxide mediated cyclization of ethyl cyanoacetate with [^{13}C]-thiourea to form [2-^{13}C]-6-amino-2-thiouracil **1**

[30]. The subsequent nitrosylation of **1** installed the ^{15}N label by electrophilic substitution using the cost-effective isotope source $Na^{15}NO_2$ to yield **2** [32]. A sodium dithionite mediated reduction of the nitroso group of **2** gave **3** and desulfurization over RANEY®-Nickel formed the diaminopyrimidone **4** [33]. Treatment of **4** with sulfuric and formic acids yielded hypoxanthine **5** [32]. Subsequent reaction of **5** with phosphorus oxychloride and N,N-dimethylaniline gave 6-chloropurine **6** which required chromatographic purification [41]. In the final step, reaction of **6** with methanolic ammonia in a microwave reactor yielded the desired adenine **7** [36]. All intermediate compounds **1-7** displayed the expected ^{1}H and ^{13}C NMR spectra reported in the literature [31, 32, 36].

We then used enzymes from the pentose phosphate and nucleotide salvage biosynthetic pathways [24, 29] to couple our newly assembled adenine **7** with D-ribose followed by subsequent phosphorylation to the corresponding ATP **8**. This one-pot enzymatic reaction was used following our previously published procedure [27] with minor alterations. In brief, ribokinase (RK, E.C. 2.7.1.15) phosphorylates the C5 position of D-ribose and then phosphoribosyl pyrophosphate synthetase (PRPPS, E.C. 2.7.6.1) pyrophosphorylates the C1 site. Adenine phosphoribosyl transferase (APRT, E.C. 2.4.2.7) then couples **7** to the 5-phospho-D-ribosyl-α-1-pyrophosphate intermediate via nucleophilic attack of adenine N9. In the final step, creatine

kinase (CK, E.C. 2.7.3.2) phosphorylates the resulting monophosphate to yield building block **8**. Complete triphosphate conversion of **7** to **8** was monitored by ^{31}P NMR and is in agreement with previous reports [42].

Taken together, our synthetic route provides **8** in a 16% overall yield with seven chemical steps and one enzymatic step and with two chromatographic purifications. This route was impacted by the low yielding (33%) formation of **5,** which resulted from complications with filtration in our hands and not with overall conversion of **4** to hypoxanthine **5**. Nevertheless, all other reactions proceeded with excellent yield to assemble the first report of an [2-^{13}C, 7-^{15}N]-ATP. What is more, our approach enables the rapid production of additional ATP building blocks by coupling **7** to different ^{2}H and/or ^{13}C-labeled D-ribose sources.

NMR spectroscopy of atom-specifically labeled RNA

Our motivation to synthesize building block **8** was for use in straightforward and accurate NMR analysis of RNA. We therefore used **8** along with unlabeled GTP, UTP, and CTP to make a 61 nt viral RNA by IVT (Fig. 1).

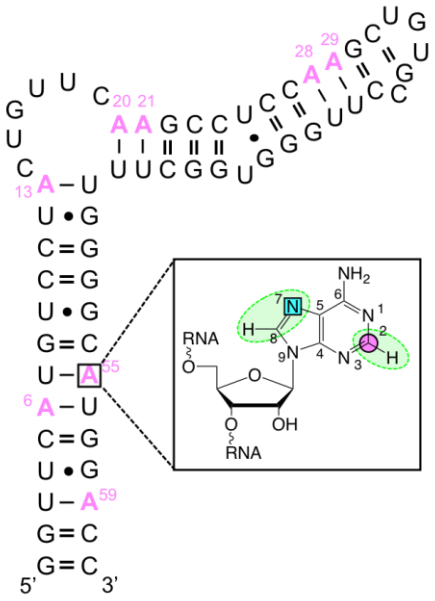

Fig. 1 Secondary structure of a 61 nt viral RNA made from IVT with building block **8** incorporated.

As a first application, we implemented 2D heteronuclear single quantum spectroscopy (HSQC) experiments using one ($^{1}J_{H2C2}$)- and two ($^{2}J_{H8N7}$)-bond couplings for coherence transfer. All eight adenosine H8-N7 resonances were clearly resolved whereas H2-C2 resonances from palindromic A6 and A55 residues showed overlap (Fig. 2a).

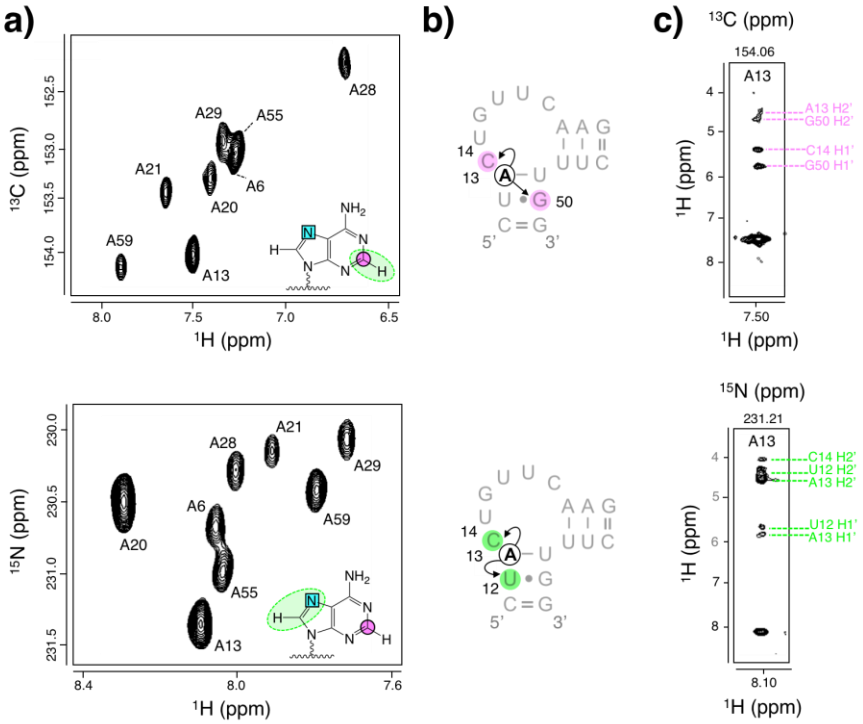

Fig. 2 HSQC and NOESY HSQC experiments in **8**-labeled RNA. **a** 2D ^{1}H,^{13}C and ^{1}H,^{15}N HSQC spectra showing H2-C2 and H8-N7 resonances. **b** Representation of NOE contacts to H2 and H8 protons for residue A13. **c** 2D ^{1}H,^{1}H slice along a single ^{13}C and ^{15}N frequency. Overlapped H1' and H2' NOE cross-peaks are resolved by the C2 and N7 chemical shift. All spectra are annotated with RNA residue assignments.

An important source of inter-proton distances for determining RNA structure by NMR spectroscopy is the nuclear Overhauser effect (NOE). Therefore, as a second application we sought to resolve ^{1}H,^{1}H NOEs into a third dimension using ^{13}C and ^{15}N edited 3D NOESY HSQC experiments to uncover all protons within ~5 Å of adenosine H2 and H8 protons. In A-helical RNA, adenosine H2 protons show cross-peaks to 3'-neighboring H1' protons on both sides of the helical strand and to their own H2' protons (Fig.

2b) [43]. Adenosine H8 protons, on the other hand, show cross peaks to 5'-neighboring H1' protons as well as to their own H1' and H2' protons (Fig. 2b) [43]. Correspondingly, we used the chemical shift of adenosine C2 and N7 to resolve NOE cross-peaks to H1' and H2' protons of H2 and H8 resonances, respectively (Fig. 2c).

As a final application, we measured dynamics in our 61 nt viral RNA. The two main dynamics parameters are the longitudinal (R_1) and transverse (R_2) relaxation rates [2]. The former measures the return of the longitudinal magnetization to thermal equilibrium whereas the latter measures the decay of x- and y- magnetization [44]. An alternative method to measure R_2 in RNA is a transverse rotating-frame ($R_{1\rho}$) experiment whereby radio frequency field pulse spin-locks the magnetization in the rotating-frame and the relaxation rate constant along the effective field is measured [2, 45]. Due to the large adenosine $^{1}J_{H2C2}$ (203 Hz) as compared to $^{2}J_{H8N7}$ (11 Hz) coupling [43], we focused on ^{13}C relaxation rates.

For uniformly [$^{13}C/^{15}N$]-ATP labeled RNAs, adenosine C2 R_1 and R_2 auto-relaxation rates include dipolar interactions with H2 and nearby ^{13}C (C4, C5, and C6) and ^{15}N (N1 and N3) nuclei (Fig. 1). Our building block **8** thereby facilitates dynamics measurements free from these unwanted dipolar couplings. To capitalize on our isolated spin pair, we used transverse relaxation optimized spectroscopy (TROSY)-detected pulse schemes to measure ^{13}C R_1 and R_2 (from $R_{1\rho}$) rates in our RNA. All adenosine C2 nuclei showed monoexponential decay and the corresponding relaxation rates were easily obtained (Fig. 3). These relaxation measurements can help identify which RNA residues are flexible or in chemical exchange and are therefore critical to understand RNA function [2].

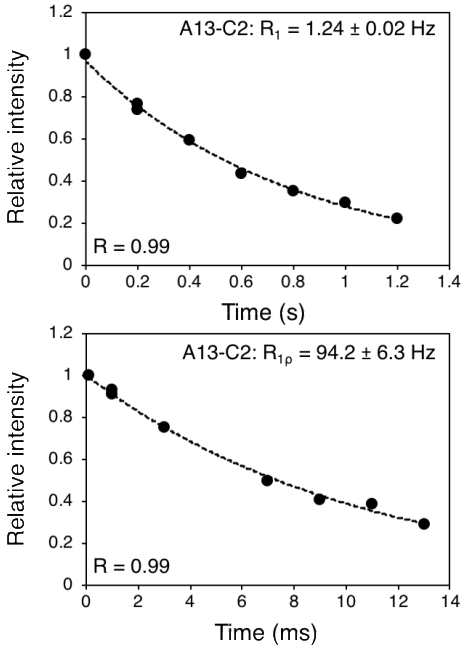

Fig. 3 Dynamics measurements in **8**-labeled RNA. Representative ^{13}C R_1 and $R_{1\rho}$ decay curves are shown for RNA residue A13. Extracted rate and curve fit are shown.

Conclusion

We report the chemo-enzymatic synthesis of an [2-^{13}C, 7-^{15}N]-ATP building block for incorporation into RNA via IVT. The atom-specifically labeled nucleobase was synthesized from cost-effective isotope sources and then converted to the corresponding ATP in a one-pot enzymatic synthesis. To showcase potential applications, we probed the structure and dynamics of a 61 nt viral RNA by solution NMR spectroscopy.

Experimental

Commercially available reagents were used throughout without further purification. Isotope labeled [^{13}C]-thiourea and [^{15}N]-sodium nitrite were purchased from Sigma Aldrich. All solvents were obtained as spectroscopic grade and used as received. All reactions sensitive to air and/or moisture were carried out under an atmosphere of argon in dry solvents using oven-dried glassware. All non-commercial enzymes used were expressed and purified in-house [29]. The microwave reaction was carried out in a CEM DiscoverTM S-class (300 W) microwave reactor with IR temperature sensor. Chromatographic purifications were carried out using silica gel or a boronate affinity resin with eluent specified. Mass spectrometric data were collected on a PerkinElmer AXION 2 TOF mass spectrometer with APCI source using ESI positive mode. ^{1}H and ^{13}C NMR spectra were recorded on a Bruker DRX 300 MHz spectrometer. ^{31}P NMR spectra were recorded on an Avance III Bruker 800 MHz spectrometer with a triple resonance cryogenic probe. Samples were maintained at a temperature of 25°C. All spectra were recorded in deuterated solvents and chemical shifts δ are reported in parts per million (ppm) relative to appropriate internal references. The following abbreviations were used to denote multiplicities: s singlet, d doublet, t triplet, m multiplet, b broad.

Synthesis

^{1}H and ^{13}C NMR spectra of compounds **1**-**7** and high-resolution mass spectrometry data for **7** can be found in the Supplemental Material. ^{31}P NMR spectra of **8** can also be found in the Supplemental Material. All α, β, and γ ^{31}P nuclei (denoted P(α), P(β), and P(γ) below) were detected, indicating successful triphosphate formation [42]. Given this, and the fact that our **8**-labeled RNA displayed the expected ^{1}H8-^{15}N7 and ^{1}H2-^{13}C2 chemical shifts of ATP [43], no further compound validation of **8** was pursued.

[2-^{13}C]-6-amino-2-thioxo-2,3-dihydropyrimidin-4(3H)-one (1, $C_3{}^{13}CH_5N_3OS$)

Sodium ethoxide (4.74 g, 69.61 mmol, 1.05 eq.) was dissolved in ethanol (150 cm^3) and then ethyl cyanoacetate (7.50 g, 66.30 mmol, 1.00 eq.) was added. Next, [^{13}C]-thiourea (5.10 g, 66.1 mmol, 1.00 eq.) was added and the suspension was refluxed at 80°C for 2 h. The solvents were removed under reduced pressure and the residual solid was dissolved in water (90 cm^3). Acetic acid was then added until pH 7 was reached to precipitate the product. The solid was vacuum filtered, successively washed with water (20 cm^3), ethanol (20 cm^3), and acetone (20 cm^3), and pure compound **1** was obtained

as a white powder. Yield: 6.76 g (71%); ^{1}H NMR (300 MHz, DMSO-d_6): δ = 11.60 (s, 1H, N(3)H), 11.51 (s, 1H, N(1)H), 6.36 (s, 2H, N(6)H2), 4.70 (s, 1H, C(5)H) ppm; ^{13}C NMR (75 MHz, DMSO-d_6): δ = 175.07 (^{13}C(2)) ppm.

[2-^{13}C, 5-^{15}N]- 6-amino-5-nitroso-2-thioxo-2,3-dihydropyrimidin-4(3H)-one (2, $C_3{}^{13}CH_4N_3{}^{15}NO_2S$)

Compound **1** (6.76 g, 46.89 mmol, 1.00 eq.) was suspended in 1 N hydrochloric acid (135 cm^3) and a solution of sodium [^{15}N]-nitrite (3.45 g, 49.23 mmol, 1.05 eq.) (41 cm^3) was added. The reaction was cooled to 0°C with an ice bath and stirred at 0°C for 5 h until a red precipitate formed. The solid was vacuum filtered and successively washed with cold water (50 cm^3) and ethanol (50 cm^3) to give pure compound **2** as a red powder. Yield: 7.35 g (90%); ^{1}H NMR (300 MHz, DMSO-d_6): δ = 12.56 (s, 1H, N(3)H), 11.23 (s, 1H, N(1)H), 7.71 (s, 2H, N(6)H2) ppm.

[2-^{13}C, 5-^{15}N]-5,6-diamino-2-thioxo-2,3-dihydropyrimidin-4(3H)-one (3, $C_3{}^{13}CH_6N_3{}^{15}NOS$)

Compound **2** (7.35 g, 42.20 mmol, 1.00 eq.) was suspended in saturated sodium bicarbonate solution (200 cm^3). The reaction was cooled to 0°C with an ice bath and solid sodium dithionite (19.10 g, 109.72 mmol, 2.60 eq.) was added in 4 equal portions at 0°C. The mixture was stirred for 6 h and then

acetic acid was added until pH 6 was reached. The resulting precipitate was vacuum filtered and successively washed with ice cold water (50 cm^3) and ethanol (50 cm^3) to give pure compound **3** as a pale yellow solid. Yield: 6.76 g (~99%); ^{1}H NMR (300 MHz, DMSO-d_6): δ = 5.68 (s, 4H, N(5)H_2, N(6)H_2) ppm.

[2-^{13}C, 5-^{15}N]- 5,6-diaminopyrimidin-4(3H)-one (4, $C_3{}^{13}CH_6N_3{}^{15}NO$)

Compound **3** (5.37 g, 33.50 mmol, 1.00 eq) was dissolved in 5% aqueous ammonia (100 cm^3) and then RANEY® nickel (20 cm^3 of a 50% slurry in water) was added. The reaction mixture was refluxed at 100°C for 2 h with vigorous stirring. The hot reaction mixture was filtered over celite and the filter cake was washed with boiling water (30 cm^3 total) several times. The filtrate was removed under reduced pressure and the residual yellow solid was co-evaporated with ethanol. Pure compound **4** was obtained as a pale yellow solid. Yield: 4.29 g (~99%); ^{1}H NMR (300 MHz, DMSO-d_6): δ = 7.41 (d, $^1J_{H2C2}$ = 200.32 Hz, 1H, ^{13}C(2)H), 5.42 (s, 4H, N(5)H_2, N(6)H_2) ppm; ^{13}C NMR (75 MHz, DMSO-d_6): δ = 140.01 (^{13}C(2)) ppm.

[2-^{13}C, 7-^{15}N]-1,9-dihydro-6H-purin-6-one (5, $C_4{}^{13}CH_4N_3{}^{15}NO$)

Compound **4** (1.75 g, 13.66 mmol, 1.00 eq.) was suspended in water (5.5 cm^3) to form a pale-yellow mixture. Then, concentrated sulfuric acid (1.34

g, 13.66, 1.00 eq) and formic acid (0.94 g, 20.49 mmol, 1.50 eq.) were successively added and the reaction was refluxed at 100°C for 19 h. The mixture was allowed to cool to room temperature and neutralized with 28% aqueous ammonia and acetic acid. The resulting red precipitate was vacuum filtered and successively washed with water (10 cm^3), ethanol (10 cm^3), and acetone (10 cm^3) to give pure compound **5** as a red solid. Yield: 0.63 g (33%); ^{1}H NMR (300 MHz, DMSO-d_6): δ = 12.56 (br, 2H, N(1)H, N(9)H), 8.12 (d, 1H, C(8)H) 7.98 (d, $^1J_{H2C2}$ = 204.56 Hz, 1H, ^{13}C(2)H) ppm; ^{13}C NMR (75 MHz, DMSO-d_6): δ = 145.10 (^{13}C(2)) ppm.

[2-^{13}C, 7-^{15}N]-6-chloro-9H-purine (6, $C_4{}^{13}CH_3ClN_3{}^{15}N$)

Compound **5** (0.63 g, 4.53 mmol, 1.00 eq.) was dissolved in $POCl_3$ (16.7 cm^3) and N,N-dimethylaniline (1.4 cm^3) and the mixture was refluxed at 150°C for 30 min. The resulting black solution was allowed to cool to room temperature and the solvent was removed under reduced pressure to form a black gum. Excess of $POCl_3$ was removed under high vacuum. The residual oil was dissolved in 25% aqueous ammonia (6 cm^3), silica gel (1.0 g) was added, and the crude product was purified via column chromatography (18.0 g, SiO_2, ((CH_2Cl_2/MeOH = 7/3 (v/v)) to obtain pure compound **6** as a brown solid; Yield: 0.71 g (~99%); R_f: 0.90 ($CHCl_3$/MeOH = 9/1 (v/v)); ^{1}H NMR (300 MHz, DMSO-d_6): δ = 8.75 (d, $^1J_{H2C2}$ = 209.32 Hz, 1H, ^{13}C(2)H), 8.69

(d, 1H, C(8)H) ppm; ^{13}C NMR (75 MHz, DMSO-d_6): δ = 151.95 (^{13}C(2)) ppm.

[2-^{13}C, 7-^{15}N]-9H-purin-6-amine (7, $C_4{}^{13}CH_5N_4{}^{15}N$)

Compound **6** (0.71 g, 4.53 mmol, 1.00 eq.) was dissolved in 7 N methanolic ammonia (14 cm^3) and heated at 150°C in a sealed tube in a microwave reactor (300 W) for 2 h. The reaction was allowed to stand overnight at room temperature until a precipitate formed. The solution was then vacuum filtered, the filtrate was evaporated, and pure compound **7** was obtained as a red solid. Yield: 0.54 g (87%); ^{1}H NMR (300 MHz, DMSO-d_6): δ = 8.12 (d, $^1J_{H2C2}$ = 197.20 Hz, 1H, ^{13}C(2)H), 8.11 (d, 1H, C(8)H), 7.13 (s, 2H, N(6)H_2) ppm; ^{13}C NMR (75 MHz, DMSO-d_6, 25°C): δ = 152.77 (^{13}C(2)) ppm; HR-MS (ESI): *m/z* calculated for $C_4{}^{13}CH_5N_4{}^{15}N$ $[M+H]^+$ 138.06271 Da, found 138.0629 Da.

[2-^{13}C, 7-^{15}N]-(((((2R,3S,4R,5R)-5-(6-amino-9H-purin-9-yl)-3,4-dihydroxytetrahydrofuran-2-yl)methoxy)oxidophosphoryl)oxidophosphoryl)phosphonate (8, $C_9{}^{13}CH_{12}N_4{}^{15}NO_{11}P_3{}^{4-}$)

Compound **8** was enzymatically synthesized *in vitro*. The 10 cm^3 reaction was carried out in 50 mM Na_3PO_4 pH 8, 100 mM KCl, 0.2% NaN_3, 10 mM

$MgCl_2$, 10 mM DTT, 0.5 mM dATP, 0.1% BSA, 100 mM creatine phosphate (CP), 8 mM **7**, 10 mM D-ribose, 0.05 mg/cm^3 CK (E.C. 2.7.3.2), 0.01 U/mm^3 myokinase (MK, E.C. 2.7.4.3), 0.1 U/mm^3 thermostable inorganic pyrophosphatase (TIPP, E.C. 3.6.1.1), 9x10^{-6} U/mm^3 RK (E.C. 2.7.1.15), 9x10^{-6} U/mm^{3}l PRPPS (E.C. 2.7.6.1), and 9x10^{-6} U/mm^3 APRT (E.C. 2.4.2.7). The reaction was incubated at 37°C for 24 h. Crude compound **8** was purified by boronate affinity chromatography (Eluent A: 1 M triethylamine pH 9; Eluent B: acidified water pH 4), lyophilized to a powder, and resuspended in Ultrapure water. Yield: 37 mg (~90%); ^{31}P NMR (324 MHz, D_2O): δ = -5.74 (d, 1P, P(γ)), -10.92 (d, 1P, P(α)), and -21.26 (t, 1P, P(β)) ppm.

RNA preparation

RNA was prepared as previously described [17]. IVT was carried out in 40 mM Tris-HCl pH 8 (at 37°C), 1 mM spermidine, 0.01% Triton-10, 80 mg/cm^3 PEG, 0.3 μM DNA template, 1 mM DTT, 2 U/mm^3 TIPP, 1.88 mM **8**, 1.88 mM GTP, 1.88 mM UTP, 1.88 mM CTP, 7.5 mM $MgCl_2$, and 0.1 mg/cm^3 T7 RNAP. Reaction proceeded for 3 h at 37°C. DNA template was purchased from Integrated DNA Technologies. After IVT, the sample was extracted with acid-phenol:chloroform, ethanol precipitated, and purified by

preparative denaturing gel electrophoresis and electroeluted. The sample was subsequently dialyzed 3-5 times against UltraPure ddH_2O, folded in NMR buffer (10 mM Na_3PO_4, 0.02% NaN_3, 0.1 mM DSS), lyophilized, and resuspended in D_2O. The RNA sample used for NMR was 0.3 mM in 300 mm^3.

NMR spectroscopy

2D HSQC, 3D NOESY HSQC, and R_1 and $R_{1\rho}$ NMR experiments were performed on an Avance III Bruker Ultrashield Plus 600 MHz spectrometer with a room temperature triple resonance probe. For the 2D HSQC experiments, the sweep widths were set to 2.5 (^{13}C), 2.2 (^{15}N), and 4.7 (^{1}H) ppm with 64 scans and 64 transients. Carriers were centered at 150.55 (^{13}C), 230.6 (^{15}N), and 4.7 (^{1}H) ppm. The ^{13}C [46] and ^{15}N [47] edited 3D NOESY HSQC experiments were recorded using previously described pulse sequences. For the ^{13}C edited experiment, INEPT transfer delays (1/(4J)) were set to 1.2 ms which is optimal for a 203 Hz $^{1}J_{H2C2}$ coupling [43]. The sweep widths were set to 2.75 (^{13}C) and 10.0 (^{1}H) ppm. Carriers were centered at 150.55 (^{13}C), 8.0 (indirect ^{1}H), and 4.7 (^{1}H) ppm. For the ^{15}N edited experiment, INEPT transfer delays (1/(4J)) were set to 16.7 ms, which is optimal for a 15 Hz $^{2}J_{H8N7}$ coupling [43]. The sweep widths were set to 2.2

(^{15}N) and 10.0 (^{1}H) ppm. Carriers were centered at 230.6 ppm (^{15}N), 10.0 (indirect ^{1}H), and 4.7 (^{1}H) ppm. For each 3D data set, 200x64 complex point sampling matrices were used for the indirect ^{1}H and ^{13}C/^{15}N dimensions along with 96 transients and non-uniform sine-weighted Poisson-gap sampling of 10% was used [48]. TROSY-detected measurements of ^{13}C R_1 and $R_{1\rho}$ relaxation rates were adapted from previous pulse sequences [45, 49]. R_1 and $R_{1\rho}$ relaxation rates were determined by fitting intensities to a monoexponential decay and errors were estimated from duplicated delay points. For R_1 experiments, relaxation delays of 0.10, 0.20 (x2), 0.40, 0.60, 0.80, 1.00, and 1.20 s were used. For $R_{1\rho}$ experiments, relaxation delays of 1.0 (x2), 3.0, 5.0, 7.0, 9.0, 11.0, and 13.0 ms were used. The strength of spin-lock field (ω_1) was 1.882 kHz. All NMR data were collected at 25°C with a recycle delay of 1.5 s and analyzed using TopSpin 4.0 and NMRViewJ [50].

Acknowledgements This research was financially supported by NSF for labeling work (1808705 to T.K.D.). We acknowledge Dr. Serge Beaucage (FDA) for hosting L.T.O. for the synthetic work, Joshua Wilhide (UMBC) for mass spectrometric analysis, and Dr. Jeffery Davis (UMD) for helpful comments.

References

1. Fürtig B, Richter C, Wöhnert J, Schwalbe H (2003) ChemBioChem 4:936–962.
2. Marušič M, Schlagnitweit J, Petzold K (2019) ChemBioChem 20:2685–2710.
3. Dethoff EA, Chugh J, Mustoe AM, Al-Hashimi HM (2012) Nature 482:322–330.
4. Ganser LR, Kelly ML, Herschlag D, Al-Hashimi HM (2019) Nat Rev Mol Cell Biol 20: 474–489.
5. Keyhani S, Goldau T, Blümler A, Heckel A, Schwalbe H (2018) Angew Chemie Int Ed 57:12017–12021.
6. Scott LG, Hennig M (2016) Methods Enzymol 566:59–87.
7. Dayie KT (2008) Int J Mol Sci 9:1214–1240.
8. Becette O, Olenginski LT, Dayie TK (2019) Molecules 24:3476.
9. Asadi-Atoi P, Barraud P, Tisne C, Kellner S (2019) Biol Chem 400:847–865.
10. Le MT, Brown RE, Simon AE, Dayie TK (2015) Methods Enzymol 565:495–535.
11. Alvarado LJ, Longhini AP, Leblanc RM, Chen B, Kreutz C, Dayie TK (2014) Methods Enzymol 549:133–162.

12. Lu K, Miyazaki Y, Summers MF (2010) J Biomol NMR 46:113–125.
13. Liu Y, Holmstrom E, Zhang J, Yu P, Wang J, Dyba MA, Chen D, Ying J, Lockett S, Nesbitt DJ, Ferré-D'Amaré AR, Sousa R, Stagno JR, Wang YX (2015) Nature 522:368–372.
14. Batey RT, Inada M, Kujawinski E, Puglisi JD, Williamson JR (1992) Nucleic Acids Res 20:4515–4523.
15. Wyatt JR, Chastain M, Puglisi JD (1991) Biotechniques 11:764–769.
16. Nikonowicz EP, Sirr A, Legault P, Jucker FM, Baer LM, Pardi A (1992) Nucleic Acids Res 20:4507–4513.
17. Milligan JF, Uhlenbeck OC (1989) Methods Enzymol 180:51–62.
18. Thakur CS, Dayie TK (2012) J Biomol NMR 52:65–77.
19. Thakur CS, Sama JN, Jackson ME, Chen B, Dayie TK (2010) J Biomol NMR 48:179–192.
20. Johnson JE, Julien KR, Hoogstraten CG (2006) J Biomol NMR 35:261–274.
21. Hoffman DW, Holland JA (1995) Nucleic Acids Res 23:3361–3362.
22. Schultheisz HL, Szymczyna BR, Scott LG, Williamson JR (2008) ACS Chem Biol 3:499–511.
23. Schultheisz HL, Szymczyna BR, Scott LG, Williamson JR (2011) J Am Chem Soc 133:297–304.
24. Tolbert TJ, Williamson JR (1996) J Am Chem Soc 118:7929–2940.

25. Leblanc RM, Longhini AP, Le Grice SFJ, Johnson BA, Dayie TK (2017) Nucleic Acids Res 45:146.

26. Nam H, Becette O, Leblanc RM, Oh D, Case DA, Dayie TK (2020) J Biomol NMR https://doi.org/10.1007/s10858-020-00315-z.

27. Longhini AP, Leblanc RM, Becette O, Salguero C, Wunderlich CH, Johnson BA, D'souza VM, Kreutz C, Dayie TK (2015) Nucleic Acids Res 44:52.

28. Alvarado LJ, LeBlanc RM, Longhini AP, Keane SC, Jain N, Yildiz ZF, Tolbert BS, D'Souza VM, Summers MF, Kreutz C, Dayie TK (2014) ChemBioChem 15:1573–1577.

29. Arthur PK, Alvarado LJ, Dayie TK (2011) Protein Expr Purif 76:229–237.

30. Traube W (1904) Liebig's Ann Chem 331:64–88.

31. Ouwerkerk N, Boom J van, Lugtenburg J, Raap J (2002) European J Org Chem 2002:2356–2362.

32. Pagano AR, Lajewski WM, Jones RA (1995) J Am Chem Soc 117:11669–11672.

33. Sethi SK, Gupta SP, Jenkins EE, Whitehead CW, Townsend LB, McCloskey JA (1982) J Am Chem Soc 104:3349–3353.

34. Kremser J, Strebitzer E, Plangger R, Juen MA, Nußbaumer F, Glasner H, Breuker K, Kreutz C (2017) ChemComm 53:12938–12941.

35. SantaLucia J, Shen LX, Cai Z, Lewis H, Tinoco I (1995) Nucleic Acids Res 23:4913–21.
36. Battaglia U, Long JE, Searle MS, Moody CJ (2011) Org Biomol Chem 9:2227–2232.
37. Gaffney BL, Rung PP, Jones RA (1990) J Am Chem Soc 112:6748–6749.
38. Yamazaki T, Muhandiram R, Kay LE (1994) J Am Chem Soc 116:8266–8278.
39. Flodell S, Petersen M, Girard F, Zdunek J, Kidd-Ljunggren K, Rgen Schleucher J, Wijmenga S (2006) Nucleic Acids Res 34:4449–4457.
40. Lee WM (1997). N Engl J Med 337:1733–1745.
41. Bendich A, Russell PJ, Fox JJ (1954) J Am Chem Soc 76:6073–6077.
42. Nardi-Schreiber A, Sapir G, Gamliel A, Kakhlon O, Sosna J, Gomori JM, Meiner V, Lossos A, Katz-Brull R (2017) ChemComm 53:9121–9124.
43. Wijmenga SS, Van Buuren BNM (1998) Prog Nucl Magn Reson Spectrosc 32:287–387.
44. Palmer AG (2004) Chem Rev 104:3623–3640.
45. Hansen AL, Al-Hashimi HM (2007) J Am Chem Soc 129:16072–16082.
46. Dieckmann T, Feigon J (1997) J Biomol NMR 9:259–72.

47. Hoffman DW (2000) J Biomol NMR 16:165–169.

48. Hyberts SG, Takeuchi K, Wagner G (2010) J Am Chem Soc 132:2145–2147.

49. Lakomek NA, Kaufman JD, Stahl SJ, Louis JM, Grishaev A, Wingfield PT, Bax A (2013) Angew Chemie Int Ed 52:3911–3915.

50. Johnson BA, Blevins RA (1994) J Biomol NMR 4:603–614.

Figure Captions

Fig. 1 Secondary structure of a 61 nt viral RNA made from IVT with building block **8** incorporated.

Fig. 2 HSQC and NOESY HSQC experiments in **8**-labeled RNA. **a** 2D $^{1}H,^{13}C$ and $^{1}H,^{15}N$ HSQC spectra showing H2-C2 and H8-N7 resonances. **b** Representation of NOE contacts to H2 and H8 protons for residue A13. **c** 2D $^{1}H,^{1}H$ slice along a single ^{13}C and ^{15}N frequency. Overlapped H1' and H2' NOE cross-peaks are resolved by the C2 and N7 chemical shift. All spectra are annotated with RNA residue assignments.

Fig. 3 Dynamics measurements in **8**-labeled RNA. Representative ^{13}C R_1 and $R_{1\rho}$ decay curves are shown for RNA residue A13. Extracted rate and curve fit are shown.

Figure 1

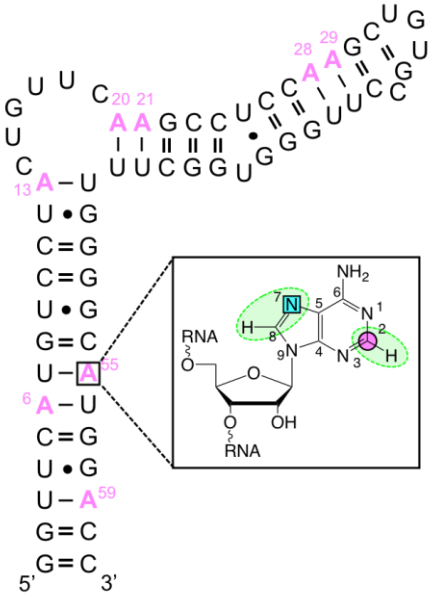

Figure 2

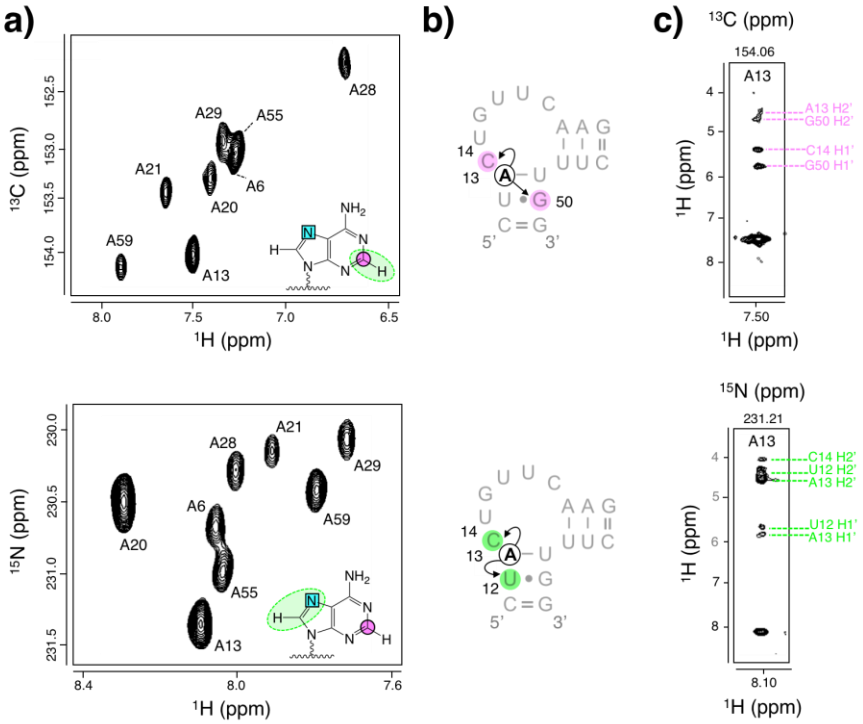

1

2

3 *Figure 3*

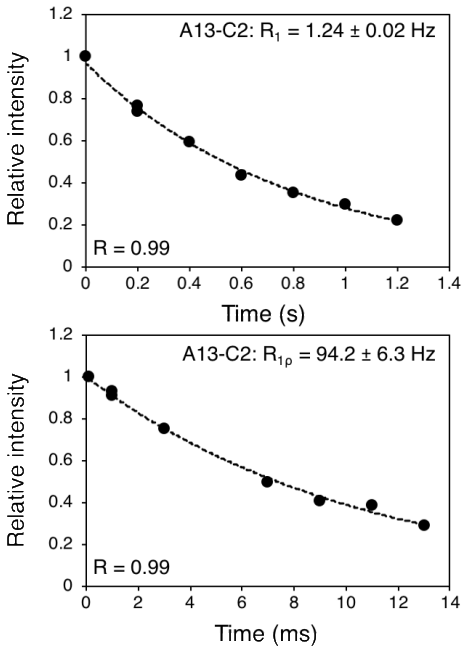

4

5

Scheme 1

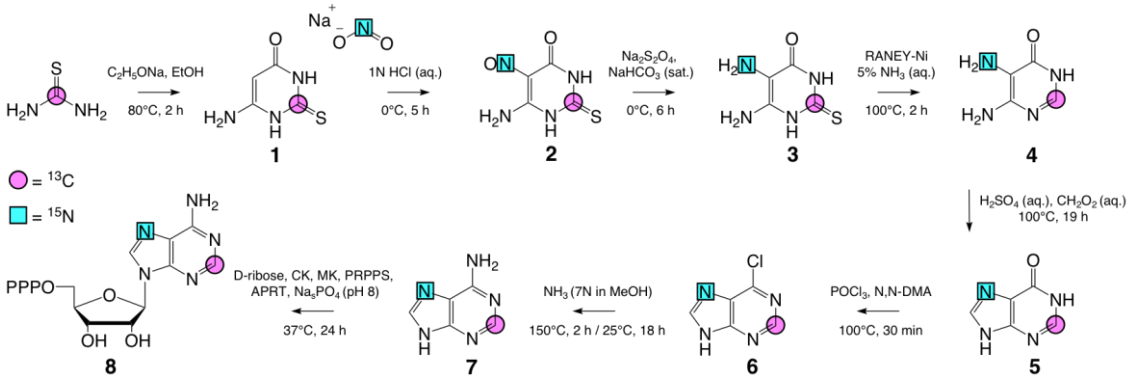

Graphical abstract